STEM CELLS AND DEVELOPMENT
Volume 20, Number 5, 2011

DOI: 10.1089/scd.2010.0362

The Ciliogenic Protein Oral-Facial-Digital 1 Regulates the Neuronal Differentiation of Embryonic Stem Cells

Julie Hunkapiller, Veena Singla, Allen Seol, and Jeremy F. Reiter

Oral-Facial-Digital 1 (OFD1) Syndrome is an X-linked developmental disorder caused by mutations in the gene *Ofd1*. OFD1 syndrome involves malformation of the face, oral cavity, and digits and may be characterized by cystic kidneys and mental retardation. Deletion or missense mutations in *Ofd1* also result in loss of primary cilia, a microtubule-based cellular projection that mediates multiple signaling pathways. *Ofd1* mutant mice display pleiotropic developmental phenotypes, including neural, skeletal, and cardiac defects. To address how loss of Ofd1 and loss of primary cilia affect early differentiation decisions, we analyzed embryoid bodies (EBs) derived from *Ofd1* mutant embryonic stem (ES) cells. *Ofd1* mutant EBs do not form primary cilia and display defects in Hedgehog and Wnt signaling. Additionally, we show that ES cells lacking Ofd1 display an increased capacity to differentiate into neurons. Nevertheless, neurons derived from *Ofd1* mutant ES cells fail to differentiate into V3 interneurons, a cell type dependent on ciliary function and Hedgehog signaling. Thus, loss of Ofd1 affects ES cell interpretation of developmental cues and reveals that EBs model some aspects of ciliopathies, providing insights into the developmental origins of OFD1 syndrome and functions of cilia.

Introduction

Cilia participate in a broad range of developmental events and organ functions [1–4]. For example, cilia are necessary for normal development of the brain, heart, kidney, limbs, and skeleton as well as for sight, hearing, and smell [1,4,5]. Further, genes involved in primary cilia formation have been found to participate in multiple signaling pathways, such as those that transduce Hedgehog (Hh), Wnt, and platelet-derived growth factor (PDGF) signals [1–3,6].

Hh signal transduction is mediated through the primary cilium, and localization of several Hh pathway components to primary cilia is necessary for their function. Smoothened, a 7-pass transmembrane protein, moves into the primary cilium in the presence of Sonic Hh (Shh) [7]. Gli proteins, the effectors of the Hh pathway, also localize to the primary cilium, and this localization is essential for formation of both activator and repressor forms [8]. Smoothened translocation to the cilium triggers the switch from formation of Gli repressors to Gli activators [8–11]. Gli3, for example, is processed to a truncated repressor form in the absence of Hh ligand [12–15]. This processing is inhibited by pathway activation in a cilium-dependent manner [8,10,11]. Gli proteins are presumed to shuttle from the cilium to the nucleus to control transcription of Hh target genes. Thus, the cilium coordinates multiple steps of the Hh pathway to regulate Hh pathway transcriptional activity.

As cilia play diverse roles in development and signaling, ciliary dysfunction manifests as human genetic syndromes known as ciliopathies, which include Meckel, Joubert, Senior-Loken, Bardet-Biedl, and Oral-Facial-Digital 1 (OFD1) syndromes [2–4,16–20]. OFD1 syndrome is characterized by polydactyly and deformity of the oral cavity and face and is caused by mutations in the gene *Ofd1* [20,21]. *Ofd1* encodes a protein that localizes to the distal end of centrioles where it functions as a cap to regulate centriole length [22,23]. As *OFD1* is X-linked, males lacking OFD1 do not form cilia, resulting in prenatal lethality [22]. The developmental phenotypes displayed in *Ofd1* mutant mice resemble those seen in humans with OFD1. Likewise *Ofd1* mutant mice share many developmental abnormalities with other mouse mutants lacking cilia [24–27]. We recently described a mouse embryonic stem (ES) cell line that contains a gene trap insertion into the gene *Ofd1* ($Ofd1^{Gt}$) [23,28]. The $Ofd1^{Gt}$ ES cell line is male and thus lacks both Ofd1 and primary cilia.

ES cells are derived from the inner cell mass of the blastocyst and can differentiate into all cell types of the body [29–31]. In addition to representing a potential for stem cell-based therapies, ES cells are a tool for investigating cell fate decisions and the mechanisms of development [31,32]. Mouse ES cells are able to maintain their pluripotency in culture by activation of the Janus kinase/signal transducers and activators or transcription (JAK/STAT) and bone morphogenic protein (BMP) pathways [33]. Upon differentiation

Department of Biochemistry and Biophysics, Cardiovascular Research Institute, University of California, San Francisco, San Francisco, California.

in suspension culture, ES cells form aggregates called embryoid bodies (EBs) [34,35]. EBs form 3 layers comprised of endoderm, mesoderm, and ectoderm and have the potential to form nearly all cell types of the embryo. [31,34,35].

Here, we used the *Ofd1*^{Gt} ES cell line to address the role of Ofd1 and primary cilia in ES cell differentiation. We found that *Ofd1*^{Gt} EBs have Hh signaling defects and exaggerated β-catenin-dependent pathway activation in response to Wnt3a. Further, differentiated *Ofd1*^{Gt} ES cells displayed increased neural differentiation. Examination of mouse mutant embryos lacking cilia demonstrated that cilia do not limit neural differentiation in vivo. Nevertheless, *Ofd1*^{Gt} EBs do not form V3 interneurons similarly to mouse mutants with abrogated ciliogenesis. V3 interneurons require high levels of Hh signaling in the ventral neural tube for induction, thus indicating that the role of cilia in EB differentiation recapitulates the role of cilia in Hh-mediated neuronal patterning.

Materials and Methods

Tissue culture

Embryonic stem cells and EBs were grown as described previously [23,28]. For Hh pathway activation, wild-type and *Ofd1*^{Gt} (RRF427; Bay Genomics) EBs were cultured for 7 days and incubated with recombinant Shh (1 μM; R&D Systems) or SAG (0.1 μM; Axxora) for 8, 18, or 24 h. Similarly, Wnt pathway activation was performed by incubating EBs for 2–4 days and adding recombinant Wnt3a (0.1 μg/mL; R&D Systems) for 4 h. BMP4 (0.1 μM; R&D Systems) and Noggin (1 μM; jCBS) were added to EBs for 48 h after being cultured for 3–6 days.

Lentiviral infection

ES cells were trypsinized and incubated for 1 h with concentrated lentivirus for either pSico-Smad1-puro or pSico-puro empty vector (gifts of Drs. Rik Derynck and Michael McManus). The cells were plated overnight and placed under selection the following morning using 2 μM puromycin. Resistant cells were selected for 5 days and knockdown was assayed. Two different Smad RNAi lentiviruses were used and gave similar results.

Immunofluorescence

For wholemount EBs. EBs were grown for 10–12 days in low suspension culture and subsequently plated onto chamber slides coated with poly-lysine and Matrigel (BD) for 48 h. EBs were washed and fixed with 4% paraformaldehyde (PFA) for 20 min and washed 3 times with phosphate buffered saline with 0.1% Triton X-100 (PBT). Subsequently, the EBs were exposed to primary block (2% bovine serum albumin and 1% serum in PBT) for 1 h. Primary antibody was added overnight in primary block at 4°C. The next day, EBs were washed and secondary block (2% bovine serum albumin and 10% serum in PBT) was added for 1 h. The EBs were then incubated with secondary antibodies for 1–2 h followed by washes with PBT. Nuclei were stained with 4′,6-diamidino-2-phenylindole in primary block for 20 min and washed again with PBT 3 times. Slides were mounted and left overnight to dry.

For embryo and EB sections. Embryos and EBs were fixed for 1 h in 4% PFA, washed, and imbedded in OCT tissue-freezing medium (OCT Tissue-Tex). The blocks were sectioned on a Microm HM 550 (Thermo-Fisher) at 12 μm thickness. The slides were washed 3 times with PBS and stained using the protocol above, except for the cilia staining protocol, which included a 2 min 100% methanol fixation.

For blastocysts. Blastocysts were flushed from the uterus at E3.5 and immunofluorescently analyzed similarly to the wholemount EBs.

All images were taken on a Nikon C1si Spectral confocal microscope.

Antibodies

The following antibodies were used for immunofluorescence and immunoblotting at the following dilutions: mouse anti-γ-tubulin (1:500; Abcam GTU488); mouse anti-Tuj1 (1:500; Covance MMS435); rabbit anti-Tuj1 (1:2,000; Covance PRB435); mouse anti-Nestin (1:300; BD Pharmingen 556309); mouse anti-Islet1/2 (1:50; DSHB); mouse anti-Nkx2.2 (1:20; DSHB); rabbit anti-β-actin (1:5,000; Abcam); rabbit anti-phospho-Smad 1/5 (1:1,000; Cell Signaling); rabbit anti-phospho-Smad 1/5/8 (1:1,000; Chemicon); rabbit anti-Rootletin (1:20,000; gift from Tiansen Li); mouse anti-acetylated tubulin (1:500; Sigma); rabbit anti-Ofd1 (1:5,000); mouse anti-α-tubulin (1:5,000). The mouse anti-Neurogenin2 antibody (1:100) was a gift from Dr. D. J. Anderson. Rabbit anti-Arl13b (1:500) was a gift from Dr. Tamara Caspary. Mouse anti-Gli3 and guinea pig anti-Gli2 were gifts from Drs. Suzie Scales (Genentech) and Jonathan Eggenschwiler, respectively, and were used at (1:4,000).

Quantitative real-time polymerase chain reaction

RNA was extracted from EBs at indicated time points using Qiagen RNeasy Plus Mini kit. RNA was then subjected to first-strand cDNA synthesis using iScript (Biorad or Fermentas). Expression levels were then analyzed in triplicate using a 7300 real-time polymerase chain reaction machine (Applied Biosystems) and normalized to β-actin. The following primers were used:

β-actin F: CACAGCTTCTTTGCAGCTCCTT
β-actin R: CGTCATCCATGGCGAACTG
Nestin F: TTAAGGCCAGAACCCCCAC
Nestin R: CTCTGCATTTTTAGGATAGGGAGC
Hnf4 F: CAGACGTCCTCCTTTTCTTGTGATA
Hnf4 R: TGTTTGGTGTGAAGGTCATGATTA
T-brachyury F: CTGGGAGCTCAGTTCTTTCGA
T-brachyury R: GAGGACGTGGCAGCTGAGA
Keratin 18 F: CGCTTGCTGGAGGATGGA
Keratin 18 R: CTTCTGCACAGTTTGCATGGA
Sox1 F: TGAAGGAACACCCGGATTACA
Sox1 R: GCCAGCGAGTACTTGTCCTTCT
Gli1 F: CTTCACCCTGCCATGAAACT
Gli1 R: TCCAGCTGAGTGTTGTCCAG
Patched F: TGATTGTGGAAGCCACAGAAAA
Patched R: TGTCTGGAGTCCGGATGGA
CyclinD1 F: CCAAGTTCCCTAGCAAGCTG
CyclinD1 R: CTTTCATGTCACAGGGCAGA
C-myc F: CAACGTCTTGGAACGTCAGA
C-myc R: TCGTCTGCTTGAATGGACAG
Follistatin F: ACGTGTGAGAACGTGGACTG
Follistatin R: CATTCGTTGCGGTAGGTTTT

Axin2 F: CTCCCCACCTTGAATGAAGA
Axin2 R: ACTGGGTCGCTTCTCTTGAA
Ngn2 F: GCTGTGGGAATTTCACCTGT
Ngn2 R: AAATTTCCACGCTTGCATTC
Tuj1 F: TGAGGCCTCCTCTCACAAGT
Tuj1 R: CGCACGACATCTAGGACTGA
Sox3 F1: CGTAACTGTCGGGGTTTTGT
Sox3 F2: CACAACTCCGAGATCAGCAA
Sox3 R1: AACCTAGGAATCCGGGAAGA
Sox3 R2: GTCCTTCTTGAGCAGCGTCT

Western immunoblot

Cells were lysed in RIPA lysis buffer with protease and phosphatase inhibitor, and protein concentration was measured. For immunoprecipitate, 0.5 μg of rabbit anti-Ofd1 antibody was added to 400 μg protein lysate overnight and bound to rProtein G agarose (Invitrogen). Samples were run on a 9% polyacrylamide gel and transferred to a polyvinylidene fluoride (PVDF) membrane. The membrane was blocked in 5% milk and incubated with primary antibody overnight at 4°C. The next day the membrane was washed and probed with secondary for 1 h. After 3 washes, the membrane was incubated with chemiluminescent substrate for 1 min and exposed for 1–30 min.

Fluorescence-activated cell sorting

EBs were grown for 10–18 days and dissociated using collagenase/dispase (1 mg/mL) for 10 min followed by 0.25% trypsin with Dnase I (1 mg/mL) for 10 min. Cells were resuspended in EB media, washed with PBS, and fixed in 2% PFA for 15 min permeabilized with 1% saponin for 15 min. Cells were resuspended in primary block (3% goat serum in PBS) for 15 min and incubated with primary for 2 h, followed by washing and incubation with secondary antibody for 1 h. Samples were washed several more times and transferred to flow cytometry tubes. Analysis was performed using a fluorescence-activated cell sorting (FACS) Calibur Flow Cytometer (BD) and FlowJo software (Treestar).

In situs. Protocol used for in situs has been described previously [36].

Cell proliferation by bromodeoxyuridine incorporation

ES cells were plated in 24-well low-suspension plates, grown for 7 days, and analyzed using the Cell Proliferation ELISA bromodeoxyuridine kit (Roche). Absorbance measured in triplicate.

Results

To understand how Ofd1 and primary cilia contribute to cell fate decisions and to establish whether ES cells may be an appropriate model system to address ciliary function, we examined whether differentiated ES cells possess primary cilia. Wild-type ES cells were grown in nonadherent suspension culture in the absence of leukemia inhibitory factor (LIF) to form EBs. When probed for Arl13b, a ciliary component, and γ-tubulin, a centrosomal component, wild-type EBs displayed abundant cilia associated with centrosomes (Fig. 1A and Supplementary Fig. S1A; Supplementary Data are available online at www.liebertonline.com/scd). While ~15% of asynchronously dividing ES cells have cilia, quantification of EB cilia showed that 28% of EB cells possess cilia at day 7 of differentiation (data not shown) [23]. Cilia were especially evident at the periphery of the EBs (Supplementary Fig. S1A).

Given that wild-type EBs possess cilia, we addressed whether *Ofd1*^{Gt} EBs, which do not make Ofd1 protein, lack primary cilia like their ES cell counterparts (Fig. 1B) [23]. Indeed, primary cilia were completely absent in the *Ofd1*^{Gt} EBs, although centrosomes were present (Fig. 1A and Supplementary Fig. S1B).

Previous studies have found that mutations that disrupt primary cilia abrogate vertebrate Hh signaling and can alter Wnt signaling [10,24,37]. To ascertain whether *Ofd1*^{Gt} EBs also display signaling abnormalities, we analyzed Gli processing and gene induction in the presence of either SAG, a small molecule activator of the Hh pathway, or Wnt3a [38]. Efficiency of Gli3 processing was assessed by measuring levels of truncated Gli3 compared with full-length Gli3. SAG induction in wild-type EBs caused increased full-length Gli3 and reciprocally decreased truncated Gli3, indicating that pathway activation inhibits Gli3 processing to the repressor form in EBs (Fig. 1C and Supplementary Fig. S1C). In contrast, addition of SAG failed to change the amount of full-length or truncated Gli3 in *Ofd1*^{Gt} EBs (Fig. 1C and Supplementary Fig. S1C). Interestingly, *Ofd1*^{Gt} EBs displayed higher levels of full-length Gli3 and Gli2 protein compared with wild-type EBs (Fig. 1C and Supplementary Fig. S1C). Together, these results indicate that *Ofd1*^{Gt} EBs display defects in Gli processing and degradation.

To determine whether *Ofd1*^{Gt} EBs generate a transcriptional response to Hh pathway stimulation, we assayed downstream target genes, *Gli1* and *Patched1* (*Ptch1*), in the presence of Hh ligand. Wild-type EBs exhibited a nearly 3-fold increase in *Gli1* and *Ptch* expression upon induction with Shh, whereas *Gli1* and *Ptch* levels in the *Ofd1*^{Gt} EBs remained the same (Fig. 1D). Notably, the increased full-length Gli3 and Gli2 protein levels observed in *Ofd1*^{Gt} EBs did not correlate with increased activity, indicating that this stabilized protein is unable to activate the Hh transcriptional program. These data indicate that *Ofd1*^{Gt} EBs, like mouse mutants lacking cilia, cannot activate genes in response to Shh.

At least some genes essential for cilium formation are required to restrain canonical Wnt signaling in mice and mouse embryonic fibroblasts [37,39]. Therefore, we assessed whether *Ofd1*^{Gt} EBs display increased responsiveness to Wnt3a. We exposed wild-type and *Ofd1*^{Gt} EBs to recombinant Wnt3a and assayed for transcriptional activation of Wnt target genes, *C-myc*, *CyclinD1*, *Axin2*, and *Follistatin*. Addition of Wnt3a in wild-type EBs induced a response in each gene, but stimulation in *Ofd1*^{Gt} EBs with equal concentrations of Wnt3a induced a greater increase in gene expression (Fig. 1E). Thus, *Ofd1*^{Gt} EBs overactivate canonical Wnt target genes in the presence of Wnt3a, similar to *Kif3a* mutant cells [37].

As Ofd1, cilia, and Hh and Wnt signaling are all critical for mammalian development, we examined how Ofd1 influences ES cell differentiation [40–42]. We analyzed expression of a panel of differentiation markers in wild-type and *Ofd1*^{Gt} EBs. Whereas markers of epithelium (*K18*), trophectoderm

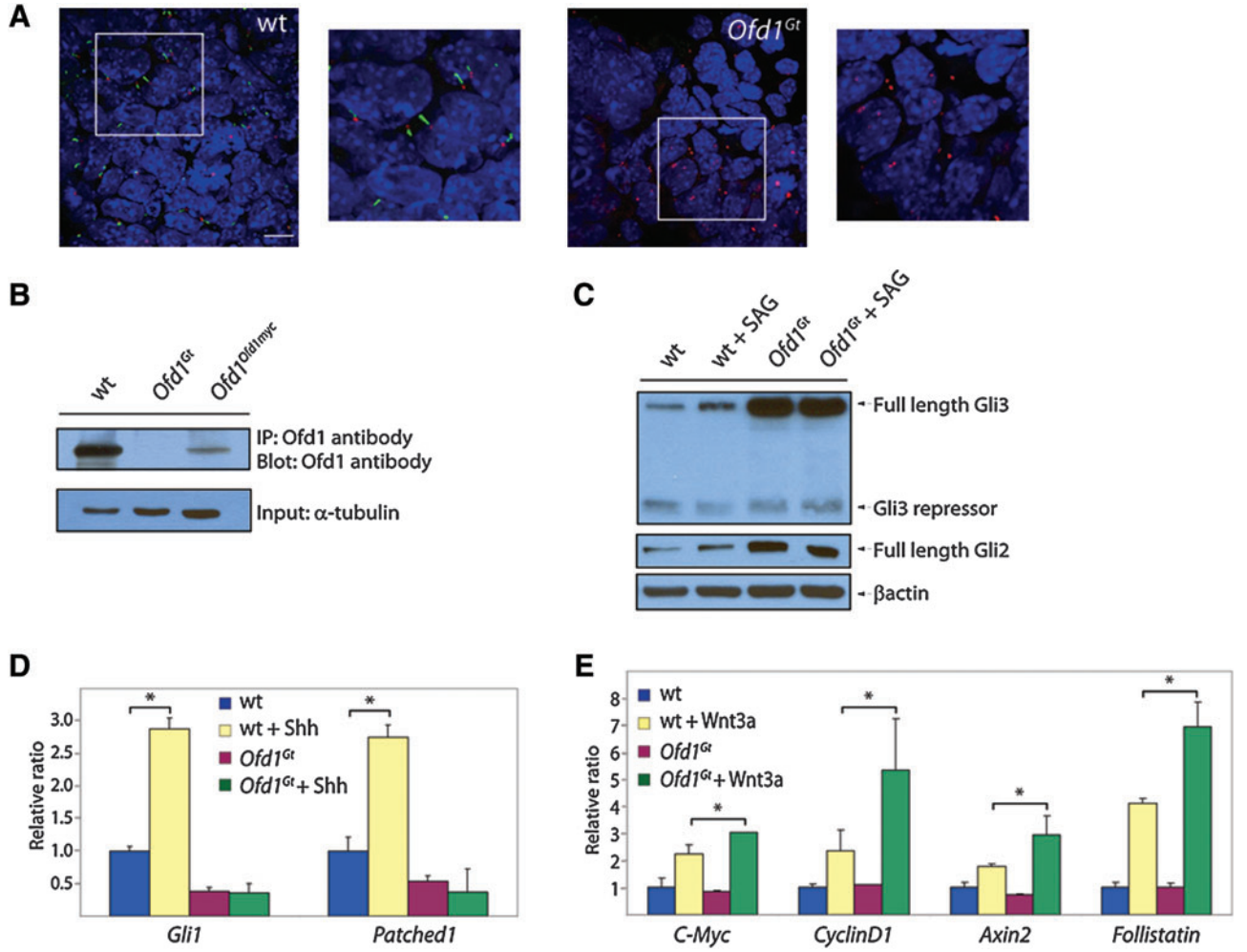

FIG. 1. *Ofd1*^{Gt} EBs lack cilia and display altered Hh and Wnt signaling. **(A)** Wild-type and *Ofd1*^{Gt} EBs stained for primary cilia (Arl13b, green), basal bodies (γ-tubulin, red), and nuclei (DAPI, blue). Scale bar 10 μm. **(B)** Immunoblot of Ofd1 from wild-type, *Ofd1*^{Gt}, and *Ofd1*^{Ofd1myc} EBs after 6 days of differentiation. **(C)** Immunoblot of wild-type and *Ofd1*^{Gt} EBs assayed for Gli3, Gli2, and β-actin after SAG or vehicle treatment for 8 h at 7 days of differentiation. **(D)** Expression levels as determined by qRT-PCR of Hh target genes *Gli1* and *Patched1* in wild-type and *Ofd1*^{Gt} EBs after addition of Shh for 18 h at 8 days of differentiation. **(E)** Expression levels as determined by qRT-PCR of Wnt target genes *C-myc*, *CyclinD1*, *Axin2*, and *Follistatin* in wild-type and *Ofd1*^{Gt} EBs grown for 2–4 days and treated with Wnt3a for 4 h. Asterisk indicates statistical significance of $p \leq 0.05$. wt, wild type; *Ofd1*, Oral-Facial-Digital 1; *Ofd1*^{Gt}, gene trap insertion into the gene *Ofd1*; EB, embryoid body; DAPI, 4′,6-diamidino-2-phenylindole; *Ofd1*^{Ofd1myc}, carboxy-terminal Myc tagged Ofd1 allele reintroduced into the endogenous locus; qRT-PCR, quantitative real-time polymerase chain reaction; Shh, sonic hedgehog. Color images available online at www.liebertonline.com/scd

(*Eomes*), and endoderm (*Hnf4*) were expressed at similar levels in wild-type and *Ofd1*^{Gt} EBs, *Ofd1*^{Gt} EBs expressed less *T-Brachyury*, an early mesodermal marker, than wild-type EBs (Fig. 2A). The most pronounced difference, however, was the increased expression of *Sox1*, a marker of neural precursors, in *Ofd1*^{Gt} EBs compared with wild-type EBs (Fig. 2A). Expression analysis of several other neural markers, including *Sox3*, *Nestin*, *Tuj1*, and *Ngn2*, also revealed a dramatic increase in *Ofd1*^{Gt} EBs, revealing a 5–35-fold change between *Ofd1*^{Gt} and wild-type EBs (Fig. 2B). These data suggest that in the absence of Ofd1, ES cells have an increased capacity to differentiate toward the neural lineage.

To test whether increased neural induction was associated with loss of Ofd1 protein or whether it was due to Ofd1-independent differences in the mutant cell line, we made use of a carboxy-terminal Myc-tagged Ofd1 allele reintroduced into the endogenous locus (*Ofd1*^{Ofd1myc}) [23,28]. The *Ofd1*^{Ofd1myc} ES cells display lower levels of Ofd1 protein than wild-type and approximately half the number of cilia (Fig. 1B and Supplementary Fig. S1B). Correlatively, *Ofd1*^{Ofd1myc} EBs express levels of neural markers intermediate to wild-type and *Ofd1*^{Gt} EBs (Fig. 2A, B). Thus, by re-expressing *Ofd1* at lower levels than wild type, we were able to partially rescue the phenotypes seen in the *Ofd1*^{Gt} EBs, suggesting that the increased neural differentiation observed in *Ofd1*^{Gt} EBs is due to loss of Ofd1 protein and primary cilia.

To distinguish whether increased neural marker expression observed in *Ofd1*^{Gt} EBs is a result of the presence of more neural cells or higher expression of neural genes within a normal number of neural cells, we analyzed wild-type and *Ofd1*^{Gt} EBs by flow cytometry and immunofluorescence. We found that *Ofd1*^{Gt} EBs contained a higher percentage of neural cells as assayed by FACS for Sox1, Tuj1, and Nestin expressing cells (Fig. 2C). Likewise, we observed expanded

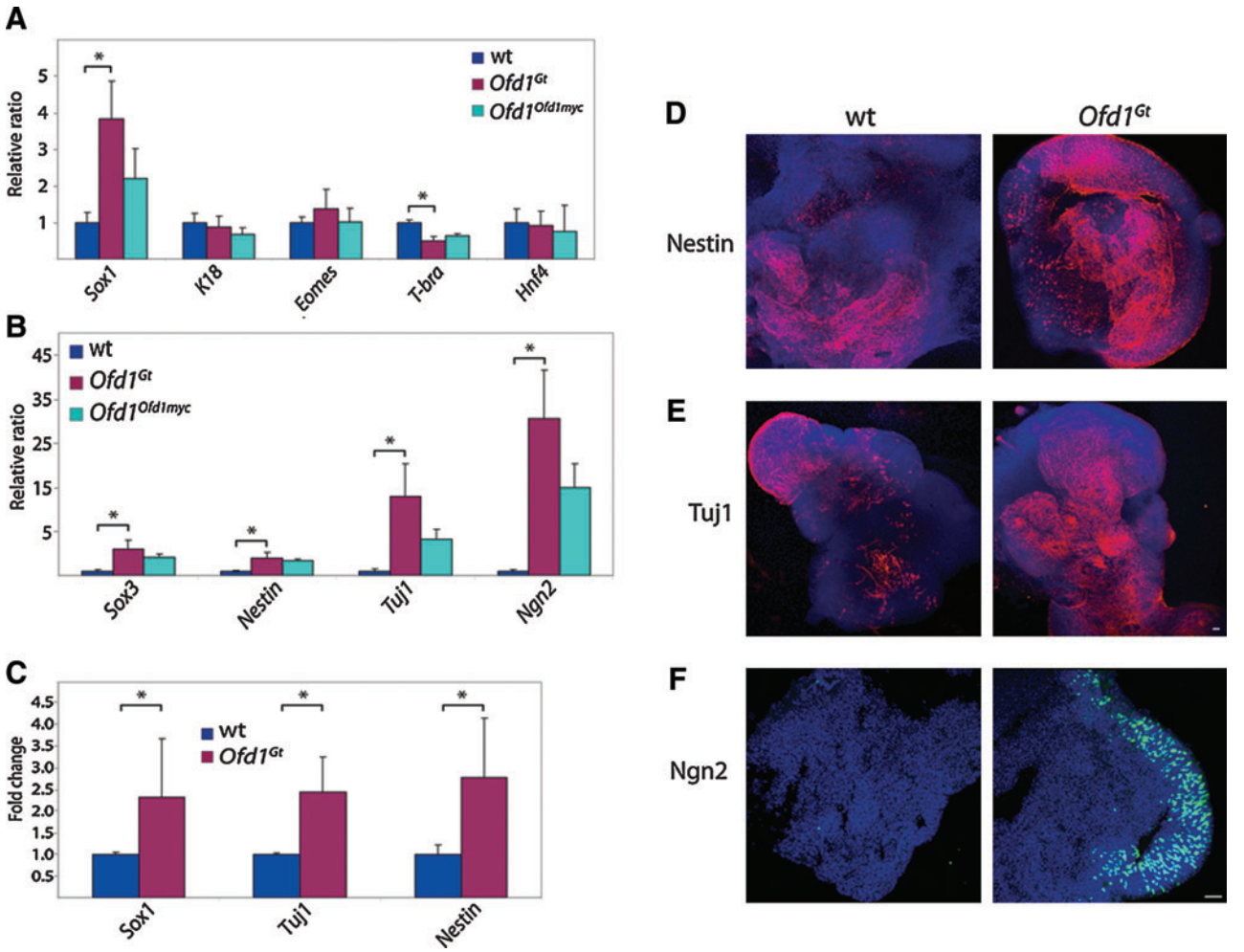

FIG. 2. *Ofd1*^{Gt} EBs exhibit increased neural differentiation. **(A)** Expression levels of tissue type markers *Sox1* (neuroectoderm), *Keratin 18* (epithelium), *Eomes* (trophectoderm), *T-brachyury* (mesoderm), and *Hnf4* (endoderm) in wild-type, *Ofd1*^{Gt}, and *Ofd1*^{Ofd1myc} EBs. **(B)** Expression levels of neural markers *Sox3*, *Nestin*, *Tuj1*, and *Ngn2* in wild-type, *Ofd1*^{Gt}, and *Ofd1*^{Ofd1myc} EBs. **(C)** Quantification of neural cells in wild-type and *Ofd1*^{Gt} EBs by fluorescence-activated cell sorting analysis of Sox1, Tuj1, and Nestin stained cells. Asterisk indicates statistical significance of $p \leq 0.01$. **(D, E)** Wholemount wild-type and *Ofd1*^{Gt} EBs stained for Nestin and Tuj1. Scale bar 20 μm. **(F)** Wild-type and *Ofd1*^{Gt} EB sections stained for Ngn2 at day 12 of differentiation. Scale bar 20 μm. Color images available online at www.liebertonline.com/scd

immunofluorescent staining of Nestin, Tuj1, and Ngn2 in *Ofd1*^{Gt} EBs compared with wild-type EBs (Fig. 2D–F). Of note, Ngn2 staining in wild-type EBs at day 12 of differentiation was dramatically lower than *Ofd1*^{Gt} EBs, whereas at later time points, wild-type EBs showed Ngn2 staining more comparable to, although still less than, *Ofd1*^{Gt} EBs (Fig. 2F and Supplementary Fig. S1D). This suggests that Ngn2 may be induced at an earlier time point in *Ofd1*^{Gt} EBs than in wild-type EBs, indicating that loss of Ofd1 changes the timing of neural differentiation.

There are several ways in which increased neural induction could occur in *Ofd1*^{Gt} EBs, including increased proliferation rates, decreased levels of apoptosis, or misregulation of cell fate decisions. Although the population-doubling rate of wild-type and *Ofd1*^{Gt} ES cells is indistinguishable, Ofd1 may impinge upon proliferation rates of differentiated cells [23]. Consequently, we tested proliferation in wild-type and *Ofd1*^{Gt} EBs by bromodeoxyuridine incorporation and phospho-histone H3 staining during differentiation. Both assays revealed that wild-type and *Ofd1*^{Gt} EBs have similar rates of cell division throughout differentiation (Fig. 3A–C). In addition, we tested levels of apoptosis by terminal deoxynucleotidyl transferase dUTP nick end labeling (TUNEL) staining, which was comparable between wild-type and *Ofd1*^{Gt} EBs (data not shown). On the basis of these data, it seems most likely that *Ofd1*^{Gt} EBs form neurons at the expense of other cell types.

Mammalian neural induction involves the interplay of several signaling pathways, including the BMP, Wnt, Nodal, fibroblast growth factor, and Hh pathways [43,44]. In particular, inhibition of the BMP pathway is a key determinant of neural fate in many vertebrates [43,45–47]. Defects in BMP pathway signaling can lead to early and increased neural induction; conversely, increased BMP signaling results in loss of forebrain development [48,49]. Thus, we tested BMP activity and the effects of BMP activation and inhibition on neural induction in wild-type and *Ofd1*^{Gt} EBs. The BMP pathway is mediated through phosphorylation of Smad

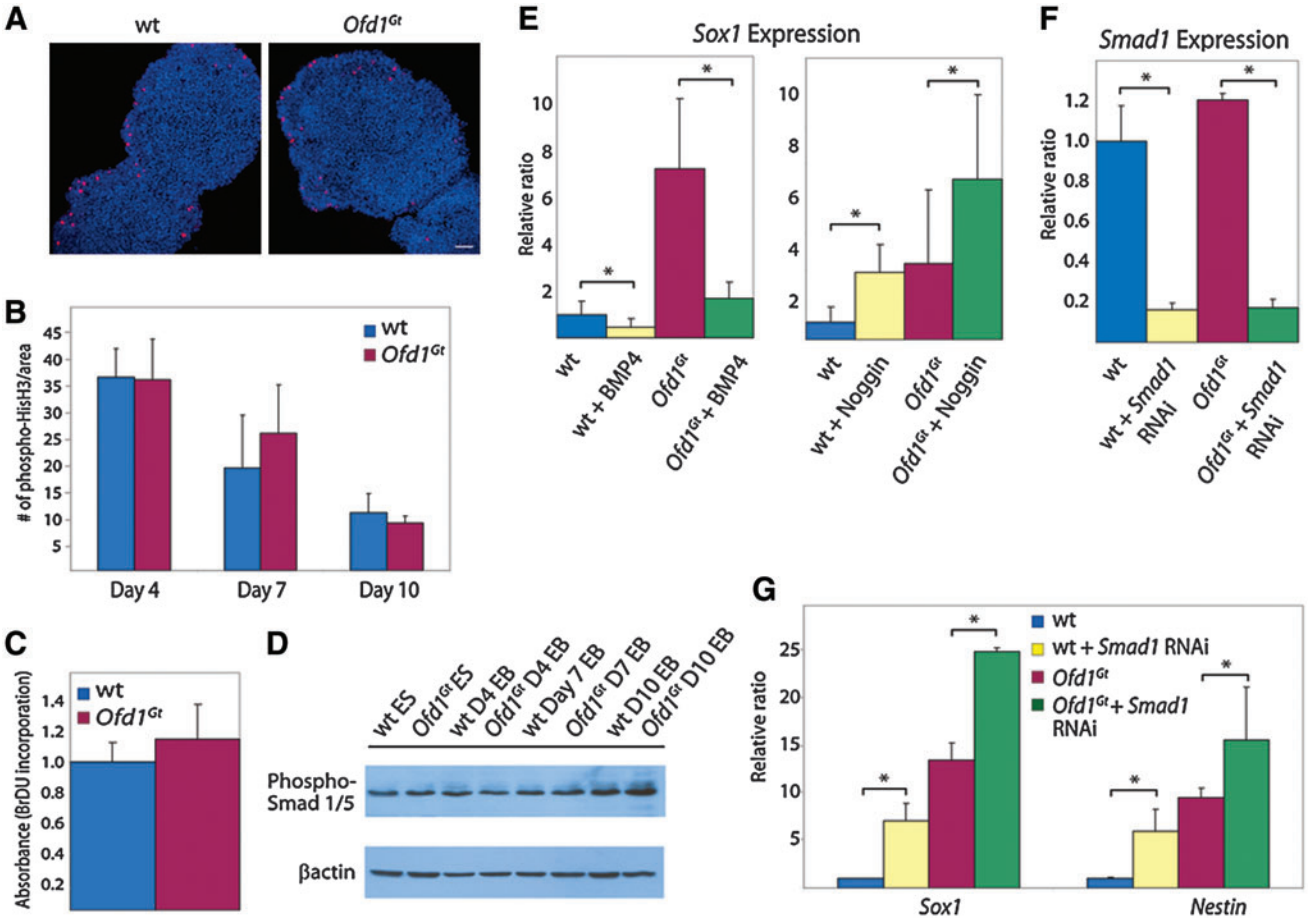

FIG. 3. Proliferation rates and BMP signaling are unaltered in *Ofd1*^{Gt} EBs. **(A)** Phospho-histone H3 staining in wild-type and *Ofd1*^{Gt} EB sections differentiated for 7 days. Scale bar 20 μm. **(B)** Quantification of phospho-histone H3 stained cells per given area of wild-type and *Ofd1*^{Gt} EBs after 4, 7, and 10 days of differentiation. **(C)** BrdU incorporation as measured by colorimetric absorbance confirming similar proliferation in wild-type and *Ofd1*^{Gt} EBs grown for 7 days. **(D)** Immunoblot of wild-type and *Ofd1*^{Gt} cells during differentiation probed for phospho-Smad 1/5 and β-actin. **(E)** Neural specification as measured by *Sox1* expression levels in wild-type and *Ofd1*^{Gt} EBs treated with BMP4 or Noggin, a BMP antagonist. **(F)** Assessment of *Smad1* knockdown in wild-type and *Ofd1*^{Gt} EBs containing *Smad1* RNAi lentivirus. **(G)** Expression of *Sox1* and *Nestin* neural markers in wild-type and *Ofd1*^{Gt} EBs treated with *Smad1* RNAi. Asterisk indicates statistical significance of $p \leq 0.05$. BMP, bone morphogenic protein; BrdU, bromodeoxyuridine. Color images available online at www.liebertonline.com/scd

proteins 1/5/8, which then bind to Smad4, relocate to the nucleus, and initiate transcription of target genes [50]. To determine whether pathway activity is altered in *Ofd1*^{Gt} EBs, levels of phosphorylated Smad1/5 were measured at time points throughout differentiation. Phosphorylated Smad levels were indistinguishable between wild-type and *Ofd1*^{Gt} EBs, suggesting that BMP activity is unaffected by loss of Ofd1 (Fig. 3D).

To further test whether increased neural induction in *Ofd1*^{Gt} EBs is due to altered responses to BMPs or BMP antagonists, we added either BMP4 or Noggin, a BMP inhibitor, to differentiating EBs and assessed neural induction. In response to BMP4, both wild-type and *Ofd1*^{Gt} EBs displayed decreased *Sox1* expression (Fig. 3E). Conversely, addition of Noggin resulted in increased Sox1 expression in wild-type and *Ofd1*^{Gt} EBs (Fig. 3E).

These results were substantiated by analyzing neural induction after interruption of the BMP pathway downstream of ligand interaction. Smad1 is a mediator of the BMP pathway as it is phosphorylated upon BMP pathway activation and translocates to the nucleus with Smad4 to activate downstream BMP target genes. Wild-type and *Ofd1*^{Gt} ES cells were transduced with a *Smad1* RNAi lentivirus and subsequently differentiated. Both wild-type and *Ofd1*^{Gt}-transduced EBs exhibited >80% knockdown of *Smad1* RNA levels and increased *Sox1* and *Nestin* expression compared with control EBs (Fig. 3F, G). On the basis of these data, BMP activity and response do not appear to depend upon Ofd1 as wild-type and *Ofd1*^{Gt} EBs react to pathway activation and inhibition similarly.

Ofd1^{Gt} EBs have defects in Hh and Wnt signaling that are similar to mouse mutants lacking Kif3a, a kinesin essential for ciliary formation [27,37]. Thus, we wanted to determine if there was a general role for cilia in restriction of neurogenesis. Although Kif3a has functions beyond cilia formation, many phenotypes in *Ift88*, *Kif3a*, and *Ofd1* null embryos are attributed to loss of cilia [22,25,27,37,39]. Therefore, we analyzed *Ift88* and *Kif3a* mutant embryos to determine whether

neural induction is increased. Neural marker expression was assessed in E9.5 *Kif3a* and *Ift88* mutants and compared with their wild-type littermates. Overall, there was a 30%–50% decrease in *Ngn2*, *Tuj1*, and *Nestin* expression in the *Kif3a* and *Ift88* mutants (Fig. 4A). In situs of E7.5 and E8.5 embryos probed for brain markers *Sox2*, *Krox20*, and *Engrailed* indicated that there was no appreciable difference in neural specification between wild-type and mutant embryos (Supplementary Fig. S2A–C). To examine neural differentiation in greater detail, E9.5 wild-type and *Ift88* mutant embryo neural tubes were examined for Nestin and Tuj1 (Fig. 4B). Stage-matched mutant embryonic neural tubes were comparable to wild type, indicating that neural induction is unperturbed in mice lacking cilia. Thus, it appears either that cilia do not serve as a constraint of neurogenesis in vivo as they do in EBs or that increased neural differentiation is specific to loss of Ofd1.

Loss of cilia causes decreased processing of Gli3 into Gli3 repressor in both *Ift88* and *Kif3a* mutant embryos, consistent with what is seen in the $Ofd1^{Gt}$ EBs [10,51]. To determine whether reduced levels of Gli3 repressor affect neural induction, we examined neural markers in $Gli3^{xt/xt}$ mutant embryos. Similar to the *Ift88* and *Kif3a* mutants, a 30%–50% decrease in neural marker expression was observed in $Gli3^{xt/xt}$ mutants as compared with their wild-type littermates at E9.5 (Fig. 4A). These results exclude Gli3 from mediating Ofd1-dependent effects on neural differentiation, and further indicate that the stabilized full-length Gli3 seen in the $Ofd1^{Gt}$ EBs does not function in neurogenesis.

To further dissect the differentiation potential of $Ofd1^{Gt}$ EBs, we tested whether $Ofd1^{Gt}$ EBs could form ventral neural subtypes. The ventral neural tube is patterned by Shh produced in the notochord and floor plate [52]. Mice lacking primary cilia have dorsalized neural tubes, including a loss of the most ventral neurons, V3 interneurons, and a decrease in motor neuron formation [11,16]. To determine whether this same phenotype occurs in vitro, wild-type and $Ofd1^{Gt}$ EBs were assayed for Nkx2.2, a marker of V3 interneurons. Whereas wild-type EBs showed widespread Nkx2.2 expression, $Ofd1^{Gt}$ EBs had very little or low Nkx2.2 expression

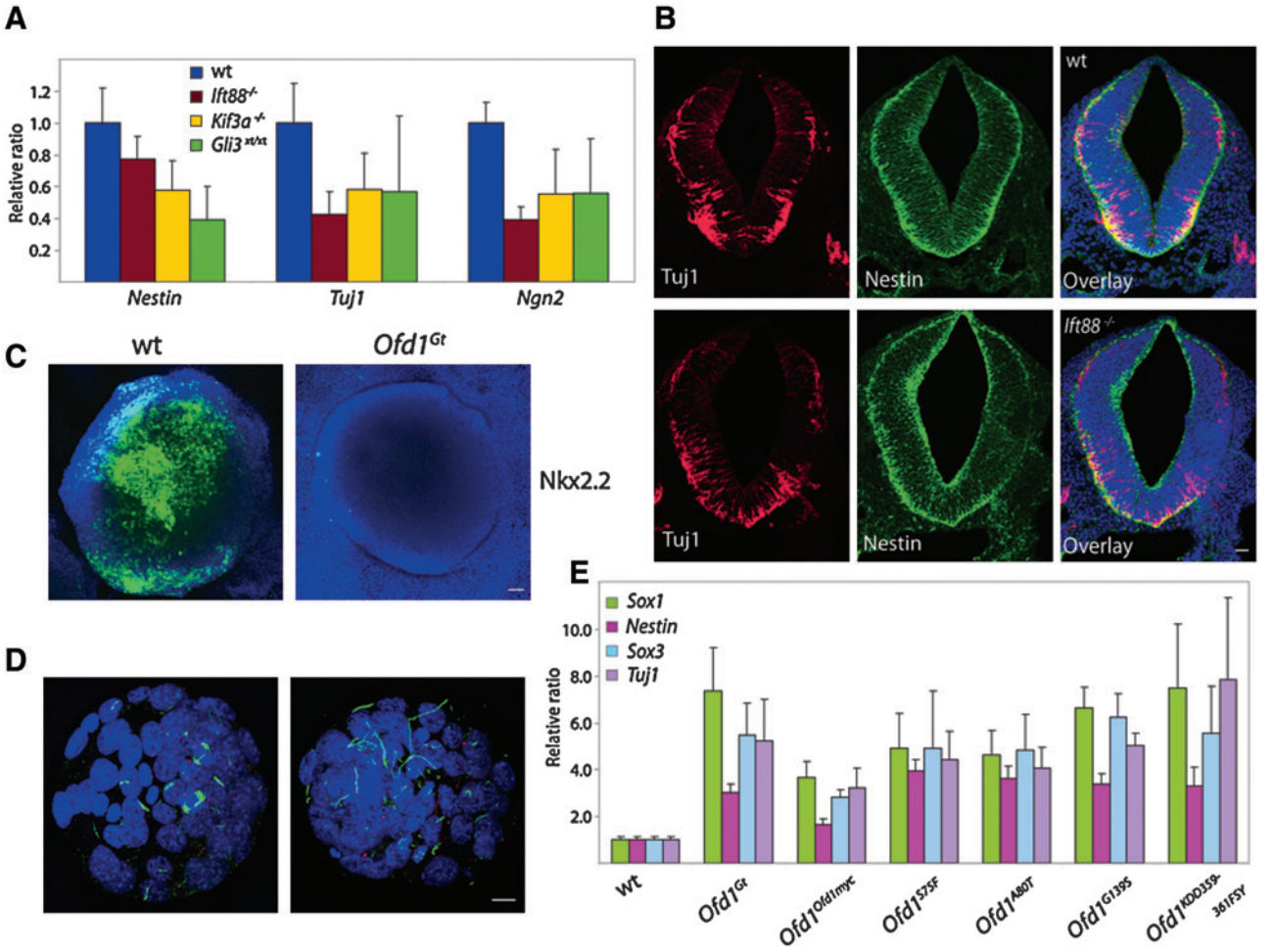

FIG. 4. Neural induction in mouse embryos lacking cilia and *Ofd1* mutant missense EBs. **(A)** Expression of neural markers *Nestin*, *Tuj1*, and *Ngn2* in E9.5 wild-type, *Ift88*, *Kif3a*, and *Gli3* mutant embryos. **(B)** Sections of E9.5 wild-type and *Ift88* mutant embryo neural tubes stained for postmitotic neurons (Tuj1, red), neural precursors (Nestin, green), and nuclei (DAPI, blue). Scale bar 20 μm. **(C)** Wholemount wild-type and $Ofd1^{Gt}$ EBs stained for Nkx2.2. Scale bar 20 μm. **(D)** Wild-type blastocysts stained for cilia (acetylated tubulin, green), basal bodies (Rootletin, red), and nuclei (DAPI, blue). Scale bar 10 μm. **(E)** qRT-PCR quantification of *Sox1*, *Nestin*, *Sox3*, and *Tuj1* expression in *Ofd1* missense mutant EBs. All expression changes between Ofd1 missense mutant and $Ofd1^{Ofd1myc}$ EBs are significant ($p \leq 0.05$). Color images available online at www.liebertonline.com/scd

(Fig. 4C). In contrast, *Ofd1*^{Gt} EBs form motor neurons at levels similar to wild-type EBs as assessed by Islet1/2 levels (Supplementary Fig. S2D). Thus, neurons that require the highest levels of Hh signaling, V3 interneurons, do not form in the absence of cilia, whereas motor neurons, which require intermediate levels, are formed in *Ofd1*^{Gt} EBs.

One reason for the disparity between the roles that cilia play in neural induction in EBs and embryos may be differences in the prevalence of cilia in EBs and mouse embryos during early development. ES cells can be ciliated and become more highly ciliated upon differentiation, whereas blastocysts, from which ES cells are derived, have not been reported to possess cilia. The first evidence of ciliation in the mouse embryo is in the embryonic node at E7.5 [53]. As differences in the prevalence of cilia could affect how ES cells and inner cell mass cells respond to signaling pathways before and during neural induction, we stained wild-type blastocysts to see if cilia were present. Most blastocysts displayed acetylated tubulin staining of mid-bodies and mitotic spindles (Fig. 4D). Moreover, we observed several blastocysts that possessed long, acetylated tubulin-containing projections, but these projections did not extend from the basal body as indicated by co-staining with Rootletin, a marker of the ciliary rootlet (Fig. 4D). As primary cilia derive from basal bodies, our interpretation is that these acetylated tubulin-positive projections are not cilia, but a distinct type of microtubular cellular structure.

Finally, to assess the effects of human disease-associated OFD1 mutations on neurogenesis, we examined whether 4 ES cell lines containing distinct OFD1-associated missense mutations in highly conserved residues or domains display defects in neural induction [23]. Although *Ofd1* missense lines, G139S and KDD359-361FSY, retain some Ofd1 protein that localizes correctly to the centrioles, all missense mutant lines show a complete or partial loss of cilia [23]. Upon differentiation, all *Ofd1* missense mutant EBs displayed increased expression levels of neural markers *Sox1*, *Nestin*, *Sox3*, and *Tuj1* compared with wild-type EBs (Fig. 4E). ES cells with mutations G139S and KDD359-361FSY are ciliated at ~20% and 35% of wild-type levels, whereas mutations S75F and A80T prohibit Ofd1 centriolar localization and cilia formation [23]. Despite differences in ciliation frequency, neural induction was relatively similar among all 4 missense mutant lines (Fig. 4E). Centrioles in the *Ofd1* missense mutant cells are structurally abnormal and lack distal appendages [23]. Thus, it is possible that the centriolar role of Ofd1 may contribute independently to its ciliogenic functions and its ability to restrain neural induction.

Discussion

Primary cilia are essential for the development of diverse tissues and organs. We have found that Ofd1 is essential for EB ciliogenesis, restrains EB neurogenesis, and is essential for V3 interneuron differentiation. These phenotypes may be attributable to the demonstrated misregulation of Hh and Wnt signaling in *Ofd1*^{Gt} EBs. However, mouse embryos lacking Ift88 or Kif3a, other proteins essential for ciliogenesis, do not show increased neural induction, raising the possibility that the neural induction defect is caused by altered centriolar structure.

To help elucidate the signaling mechanisms causing increased neural induction, we investigated the involvement of the BMP, Hh, and Wnt pathways, known regulators of neural induction and differentiation. Inhibition of the BMP pathway has been shown to be important for neural induction in diverse vertebrates, and in some species, BMP inhibition is sufficient to induce neural tissue [43,45,48,49,54]. Mammals require BMP signaling for proper neural induction, but also require inputs from additional pathways. When induced with BMP agonists or antagonists, wild-type and *Ofd1*^{Gt} EBs displayed comparable changes in neural induction, suggesting that the cilium is not essential for interpretation of BMP signals. Likewise, levels of phosphorylated Smads, the downstream mediators of BMP signaling, were similar in wild-type and *Ofd1*^{Gt} EBs, indicating that BMP pathway activity is not dependent on Ofd1 or the primary cilium. Further, disruption of the intracellular BMP signal transduction pathway using *Smad* RNAi resulted in comparable increases in neural marker expression. These experiments suggest that loss of cilia has no effect on BMP signaling, and misregulation of other pathways likely results in increased neurogenesis in *Ofd1*^{Gt} EBs.

Both Hh and Wnt signaling pathways are important for neural differentiation and specification [43,52,55]. Previous studies have shown that cells and mouse embryos lacking primary cilia have defective Hh signaling and can display overactive Wnt responsiveness [37]. Consistent with this data, we found that *Ofd1*^{Gt} EBs also have an overactive canonical response to Wnt3a. Additionally, we show that *Ofd1*^{Gt} EBs cannot activate downstream Hh target genes upon treatment with Shh and show abrogated processing of Gli3 to the truncated repressor form. Thus, *Ofd1*^{Gt} EBs recapitulate the known biochemical and transcriptional Hh signaling defects displayed by mouse embryos lacking cilia.

Despite similarities in signaling profiles between *Ofd1*^{Gt} EBs and embryos lacking cilia, we observed increased neural induction in *Ofd1*^{Gt} EBs, but not in *Ift88* or *Kif3a* mutants. One possible reason for the divergence in neural induction observed in embryos without cilia and unciliated EBs may be differences in the temporal regulation of ciliogenesis. Approximately 15% of undifferentiated ES cells are ciliated, whereas blastocysts do not appear to be. Early discrepancies in ciliation frequency could influence how signaling is mediated and consequently how cell fates are determined. Another fundamental difference between EB differentiation and embryo development is the spatial disorganization of EB tissues. During development, embryonic architecture limits the exposure of prospective neural tissue to other tissues, signals, and cell–cell contacts. These barriers are less present in the chaotic EB environment.

Variation of growth conditions could also account for neurogenesis differences between *Ofd1*^{Gt} EBs and *Ift88* and *Kif3a* mutant embryos. EBs are cultured in vitro in the presence of signaling factors than normally regulate embryo development. Nonetheless, this formula of factors may be quite distinct than the milieu found in the developing embryo.

Although Hh and Wnt signaling are abnormal in the *Ofd1*^{Gt} EBs, the effects of these two pathways on neurogenesis either alone or cooperatively is unclear. Wnt signaling is important for maintenance of neural precursors and specification of the dorsal spinal cord, whereas Shh signaling from the notochord induces neural proliferation and specifies subclasses of ventral interneurons [15,16,48,54–59]. There are, however, instances in which the Hh and Wnt pathways

coordinately regulate neural development. For example, Gli3 repressor inhibits canonical Wnt signaling by binding β-catenin during spinal cord patterning [56]. Additionally, glycogen synthase kinase 3 (GSK3), a component of both the Hh and Wnt pathways, is required for normal proliferation of neural progenitors [55]. Future studies are needed to dissect the molecular interactions of these two pathways during ES cell differentiation.

Another area of future study is to explore whether defects in primary cilia or defective centrioles may affect ES cell differentiation in distinct ways. *Ofd1* null mice show phenotypes resembling those of other mutant embryos lacking cilia, such as *Ift88* mutants, suggesting that Ofd1 functions primarily in cilium assembly. Indeed, *Ofd1* missense mutant cells lacking cilia, either partially or completely, all displayed increased neural induction. All *Ofd1* missense mutant lines also have abnormal centriolar structure, even in cases in which the mutant Ofd1 localizes properly to the distal centriole [23]. Thus, it is difficult to discern whether increased neural differentiation is a result of loss of cilia or defective centrioles. To distinguish these 2 possibilities, neural differentiation will need to be assayed in ES cells that lack cilia but have normal centriolar structure.

The neural tube is patterned by signaling molecule gradients initiated in the notochord and roof plate. V3 interneurons are the most ventral subtype, requiring the highest levels of Hh signaling for specification. Indeed, mouse mutants without cilia lack V3 interneurons and form few motor neurons due to the absence of Hh signaling. Consistent with this finding and the loss of Hh responsiveness in $Ofd1^{Gt}$ EBs, we observed few, if any, V3 interneurons in the $Ofd1^{Gt}$ EBs. In contrast, $Ofd1^{Gt}$ EBs do form motor neurons, which are induced more dorsally in the neural tube than are V3 interneurons. Given that inhibition of Gli3 repressor participates in motor neuron development, it is likely that formation of motor neurons in $Ofd1^{Gt}$ EBs is caused by decreased Gli3 processing [15,60–62]. Hence, the defects in $Ofd1^{Gt}$ EB neural specification recapitulate defects in neural tube patterning observed in mouse mutants with dysfunctional cilia.

This work demonstrates that ES cell differentiation is a useful way to study the developmental mechanisms underlying ciliopathies. Although we differentiated ES cells spontaneously in suspension culture, other protocols that direct differentiation to specific cell types such as pancreatic cells, cardiomyocytes, and motor neurons may be utilized to study the role of primary cilia in the development of specific cell types. For example, directed differentiation of $Ofd1^{Gt}$ ES cells to cardiomyocytes or neural stem cells may allow one to study how primary cilia affect stem cell maintenance or the ability to respond to stress or damage [5]. This system also potentially alleviates the need to derive and immortalize cell lines, which may facilitate correlating cell biological and embryological findings. Taken together, these results examining the role of Ofd1 and primary cilia in neural differentiation demonstrate the utility of the ES cell system to study the intricate role of cilia in developmental signaling and patterning.

Acknowledgments

The authors thank the UCSF Nikon Imagining Center at UCSF as well as the UCSF Lentiviral RNAi and FACS core. We also thank Holly Ingram for use of the 7300 Real-Time polymerase chain reaction system and members of the Reiter lab for valuable discussions. The Nkx2.2 and Islet1/2 antibodies were obtained from the Developmental Studies Hybridoma Bank developed under the auspices of the National Institute of Child Health and Human Development (NICHD) and maintained by The University of Iowa, Department of Biology, Iowa City, IA. This work was funded by grants from the California Institute for Regenerative Medicine, the National Institutes of Health (RO1AR054396), the Burroughs Wellcome Fund, the Packard Foundation, the Sandler Family Supporting Foundation, and the Helmsley Charitable Trust to J.F.R., and also by fellowships from Genentech and the California Institute for Regenerative Medicine to J.H.

Author Disclosure Statement

All authors state that no competing financial interests exist.

References

1. Singla V and JF Reiter. (2006). The primary cilium as the cell's antenna: signaling at a sensory organelle. Science 313: 629–633.
2. Gerdes JM, EE Davis and N Katsanis. (2009). The vertebrate primary cilium in development, homeostasis, and disease. Cell 137:32–45.
3. Bisgrove BW and HJ Yost. (2006). The roles of cilia in developmental disorders and disease. Development 133:4131–4143.
4. Fliegauf M, T Benzing and H Omran. (2007). When cilia go bad: cilia defects and ciliopathies. Nat Rev Mol Cell Biol 8:880–893.
5. Clement CA, SG Kristensen, K Mollgard, GJ Pazour, BK Yoder, LA Larsen and ST Christensen. (2009). The primary cilium coordinates early cardiogenesis and hedgehog signaling in cardiomyocyte differentiation. J Cell Sci 122:3070–3082.
6. Schneider L, CA Clement, SC Teilmann, GJ Pazour, EK Hoffmann, P Satir and ST Christensen. (2005). PDGFRalphaalpha signaling is regulated through the primary cilium in fibroblasts. Curr Biol 15:1861–1866.
7. Corbit KC, P Aanstad, V Singla, AR Norman, DY Stainier and JF Reiter. (2005). Vertebrate Smoothened functions at the primary cilium. Nature 437:1018–1021.
8. Haycraft CJ, B Banizs, Y Aydin-Son, Q Zhang, EJ Michaud and BK Yoder. (2005). Gli2 and Gli3 localize to cilia and require the intraflagellar transport protein polaris for processing and function. PLoS Genet 1:e53.
9. May SR, AM Ashique, M Karlen, B Wang, Y Shen, K Zarbalis, J Reiter, J Ericson and AS Peterson. (2005). Loss of the retrograde motor for IFT disrupts localization of Smo to cilia and prevents the expression of both activator and repressor functions of Gli. Dev Biol 287:378–389.
10. Liu A, B Wang and LA Niswander. (2005). Mouse intraflagellar transport proteins regulate both the activator and repressor functions of Gli transcription factors. Development 132:3103–3111.
11. Huangfu D and KV Anderson. (2005). Cilia and Hedgehog responsiveness in the mouse. Proc Natl Acad Sci U S A 102:11325–11330.
12. Sasaki H, Y Nishizaki, C Hui, M Nakafuku and H Kondoh. (1999). Regulation of Gli2 and Gli3 activities by an amino-terminal repression domain: implication of Gli2 and Gli3 as

primary mediators of Shh signaling. Development 126:3915–3924.
13. Ruiz i Altaba A. (1999). Gli proteins encode context-dependent positive and negative functions: implications for development and disease. Development 126:3205–3216.
14. Wang B, JF Fallon and PA Beachy. (2000). Hedgehog-regulated processing of Gli3 produces an anterior/posterior repressor gradient in the developing vertebrate limb. Cell 100:423–434.
15. Litingtung Y and C Chiang. (2000). Specification of ventral neuron types is mediated by an antagonistic interaction between Shh and Gli3. Nat Neurosci 3:979–985.
16. Wong SY and JF Reiter. (2008). The primary cilium at the crossroads of mammalian hedgehog signaling. Curr Top Dev Biol 85:225–260.
17. Zaghloul NA and N Katsanis. (2009). Mechanistic insights into Bardet-Biedl syndrome, a model ciliopathy. J Clin Invest 119:428–437.
18. Badano JL, N Mitsuma, PL Beales and N Katsanis. (2006). The ciliopathies: an emerging class of human genetic disorders. Annu Rev Genomics Hum Genet 7:125–148.
19. Parisi MA. (2009). Clinical and molecular features of Joubert syndrome and related disorders. Am J Med Genet C Semin Med Genet 151C:326–340.
20. Macca M and B Franco. (2009). The molecular basis of oral-facial-digital syndrome, type 1. Am J Med Genet C Semin Med Genet 151C:318–325.
21. Ferrante MI, A Barra, JP Truong, S Banfi, CM Disteche and B Franco. (2003). Characterization of the OFD1/Ofd1 genes on the human and mouse sex chromosomes and exclusion of Ofd1 for the Xpl mouse mutant. Genomics 81:560–569.
22. Ferrante MI, A Zullo, A Barra, S Bimonte, N Messaddeq, M Studer, P Dolle and B Franco. (2006). Oral-facial-digital type I protein is required for primary cilia formation and left-right axis specification. Nat Genet 38:112–117.
23. Singla V, M Romaguera-Ros, JM Garcia-Verdugo and JF Reiter. (2010). Ofd1, a human disease gene, regulates the length and distal structure of centrioles. Dev Cell 18:410–424.
24. Huangfu D, A Liu, AS Rakeman, NS Murcia, L Niswander and KV Anderson. (2003). Hedgehog signalling in the mouse requires intraflagellar transport proteins. Nature 426:83–87.
25. Pazour GJ, BL Dickert, Y Vucica, ES Seeley, JL Rosenbaum, GB Witman and DG Cole. (2000). Chlamydomonas IFT88 and its mouse homologue, polycystic kidney disease gene tg737, are required for assembly of cilia and flagella. J Cell Biol 151:709–718.
26. Nonaka S, Y Tanaka, Y Okada, S Takeda, A Harada, Y Kanai, M Kido and N Hirokawa. (1998). Randomization of left-right asymmetry due to loss of nodal cilia generating leftward flow of extraembryonic fluid in mice lacking KIF3B motor protein. Cell 95:829–837.
27. Marszalek JR, P Ruiz-Lozano, E Roberts, KR Chien and LS Goldstein. (1999). Situs inversus and embryonic ciliary morphogenesis defects in mouse mutants lacking the KIF3A subunit of kinesin-II. Proc Natl Acad Sci U S A 96:5043–5048.
28. Singla V, J Hunkapiller, N Santos, AD Seol, AR Norman, P Wakenight, WC Skarnes and JF Reiter. (2010). Floxin, a resource for genetically engineering mouse ESCs. Nat Methods 7:50–52.
29. Martin GR. (1981). Isolation of a pluripotent cell line from early mouse embryos cultured in medium conditioned by teratocarcinoma stem cells. Proc Natl Acad Sci U S A 78: 7634–7638.
30. Evans MJ and MH Kaufman. (1981). Establishment in culture of pluripotential cells from mouse embryos. Nature 292:154–156.
31. Keller G. (2005). Embryonic stem cell differentiation: emergence of a new era in biology and medicine. Genes Dev 19:1129–1155.
32. Jaenisch R and R Young. (2008). Stem cells, the molecular circuitry of pluripotency and nuclear reprogramming. Cell 132:567–582.
33. Liu N, M Lu, X Tian and Z Han. (2007). Molecular mechanisms involved in self-renewal and pluripotency of embryonic stem cells. J Cell Physiol 211:279–286.
34. Doetschman TC, H Eistetter, M Katz, W Schmidt and R Kemler. (1985). The *in vitro* development of blastocyst-derived embryonic stem cell lines: formation of visceral yolk sac, blood islands and myocardium. J Embryol Exp Morphol 87:27–45.
35. Keller GM. (1995). *In vitro* differentiation of embryonic stem cells. Curr Opin Cell Biol 7:862–869.
36. Henrique D, J Adam, A Myat, A Chitnis, J Lewis and D Ish-Horowicz. (1995). Expression of a Delta homologue in prospective neurons in the chick. Nature 375:787–790.
37. Corbit KC, AE Shyer, WE Dowdle, J Gaulden, V Singla, MH Chen, PT Chuang and JF Reiter. (2008). Kif3a constrains beta-catenin-dependent Wnt signalling through dual ciliary and non-ciliary mechanisms. Nat Cell Biol 10:70–76.
38. Chen JK, J Taipale, KE Young, T Maiti and PA Beachy. (2002). Small molecule modulation of Smoothened activity. Proc Natl Acad Sci U S A 99:14071–14076.
39. Ocbina PJ, M Tuson and KV Anderson. (2009). Primary cilia are not required for normal canonical Wnt signaling in the mouse embryo. PLoS One 4:e6839.
40. Logan CY and R Nusse. (2004). The Wnt signaling pathway in development and disease. Annu Rev Cell Dev Biol 20:781–810.
41. Veland IR, A Awan, LB Pedersen, BK Yoder and ST Christensen. (2009). Primary cilia and signaling pathways in mammalian development, health and disease. Nephron Physiol 111:p39–53.
42. Jiang J and CC Hui. (2008). Hedgehog signaling in development and cancer. Dev Cell 15:801–812.
43. Gaulden J and JF Reiter. (2008). Neur-ons and neur-offs: regulators of neural induction in vertebrate embryos and embryonic stem cells. Hum Mol Genet 17:R60–R66.
44. Munoz-Sanjuan I and AH Brivanlou. (2002). Neural induction, the default model and embryonic stem cells. Nat Rev Neurosci 3:271–280.
45. Beddington RS. (1994). Induction of a second neural axis by the mouse node. Development 120:613–620.
46. Hemmati-Brivanlou A and DA Melton. (1992). A truncated activin receptor inhibits mesoderm induction and formation of axial structures in Xenopus embryos. Nature 359:609–614.
47. Smith WC and RM Harland. (1992). Expression cloning of noggin, a new dorsalizing factor localized to the Spemann organizer in Xenopus embryos. Cell 70:829–840.
48. Bachiller D, J Klingensmith, C Kemp, JA Belo, RM Anderson, SR May, JA McMahon, AP McMahon, RM Harland, J Rossant and EM De Robertis. (2000). The organizer factors Chordin and Noggin are required for mouse forebrain development. Nature 403:658–661.
49. Di-Gregorio A, M Sancho, DW Stuckey, LA Crompton, J Godwin, Y Mishina and TA Rodriguez. (2007). BMP signalling inhibits premature neural differentiation in the mouse embryo. Development 134:3359–3369.

50. Liu A and LA Niswander. (2005). Bone morphogenetic protein signalling and vertebrate nervous system development. Nat Rev Neurosci 6:945–954.
51. Kolpakova-Hart E, M Jinnin, B Hou, N Fukai and BR Olsen. (2007). Kinesin-2 controls development and patterning of the vertebrate skeleton by Hedgehog- and Gli3-dependent mechanisms. Dev Biol 309:273–284.
52. Dessaud E, AP McMahon and J Briscoe. (2008). Pattern formation in the vertebrate neural tube: a sonic hedgehog morphogen-regulated transcriptional network. Development 135:2489–2503.
53. Sulik K, DB Dehart, T Iangaki, JL Carson, T Vrablic, K Gesteland and GC Schoenwolf. (1994). Morphogenesis of the murine node and notochordal plate. Dev Dyn 201:260–278.
54. Mukhopadhyay M, S Shtrom, C Rodriguez-Esteban, L Chen, T Tsukui, L Gomer, DW Dorward, A Glinka, A Grinberg, SP Huang, C Niehrs, JC Izpisua Belmonte and H Westphal. (2001). Dickkopf1 is required for embryonic head induction and limb morphogenesis in the mouse. Dev Cell 1:423–434.
55. Kim WY, X Wang, Y Wu, BW Doble, S Patel, JR Woodgett and WD Snider. (2009). GSK-3 is a master regulator of neural progenitor homeostasis. Nat Neurosci 12:1390–1397.
56. Ulloa F, N Itasaki and J Briscoe. (2007). Inhibitory Gli3 activity negatively regulates Wnt/beta-catenin signaling. Curr Biol 17:545–550.
57. Kelly OG, KI Pinson and WC Skarnes. (2004). The Wnt coreceptors Lrp5 and Lrp6 are essential for gastrulation in mice. Development 131:2803–2815.
58. Muroyama Y, M Fujihara, M Ikeya, H Kondoh and S Takada. (2002). Wnt signaling plays an essential role in neuronal specification of the dorsal spinal cord. Genes Dev 16:548–553.
59. Shimizu T, T Kagawa, T Inoue, A Nonaka, S Takada, H Aburatani and T Taga. (2008). Stabilized beta-catenin functions through TCF/LEF proteins and the Notch/RBP-Jkappa complex to promote proliferation and suppress differentiation of neural precursor cells. Mol Cell Biol 28:7427–7441.
60. Persson M, D Stamataki, P te Welscher, E Andersson, J Bose, U Ruther, J Ericson and J Briscoe. (2002). Dorsal-ventral patterning of the spinal cord requires Gli3 transcriptional repressor activity. Genes Dev 16:2865–2878.
61. Oh S, X Huang, J Liu, Y Litingtung and C Chiang. (2009). Shh and Gli3 activities are required for timely generation of motor neuron progenitors. Dev Biol 331:261–269.
62. Wijgerde M, JA McMahon, M Rule and AP McMahon. (2002). A direct requirement for Hedgehog signaling for normal specification of all ventral progenitor domains in the presumptive mammalian spinal cord. Genes Dev 16:2849–2864.

Address correspondence to:
Dr. Jeremy F. Reiter
Department of Biochemistry and Biophysics
Cardiovascular Research Institute
University of California, San Francisco
1550 4th Street
Rock Hall Rm 446
Box 2822
San Francisco, CA 94158

E-mail: jeremy.reiter@ucsf.edu

Received for publication August 24, 2010
Accepted after revision September 25, 2010
Prepublished on Liebert Instant Online September 27, 2010